

A reliability-based approach to the robustness of corroded RC structures

Eduardo S. Cavaco^{a,b}, Luis A. C. Neves^c, Joan R. Casas^{d,*}

^a*Civil Engineering Department, Universidade NOVA de Lisboa, Quinta da Torre, 2829-516, Monte da Caparica, Portugal*

^b*CERIS - Civil Engineering Research and Innovation for Sustainability, Av. Rovisco Pais, 1 1049-001 Lisboa, Portugal*

^c*Nottingham Transportation Engineering Centre (NTEC), Dept. of Civil Engineering, University of Nottingham, NG7 2RD Nottingham, United Kingdom*

^d*Civil Engineering Department, Technical University of Catalunya, Modulo C1, Barcelona, Spain*

Abstract

Currently, decisions on infrastructural assets maintenance and repair, in particular on structures, are based, mostly, on the results of inspections and the resulting condition index, neglecting systems robustness, and, therefore, not making optimize use of the limited available funds. This paper presents a definition and a measure of structural robustness in the context of deteriorating structures, compatible with assets management systems for optimal maintenance and repair planning. The proposed index is used in defining the robustness of existing RC structures to rebar corrosion. Structural performance and the corresponding reliability index are assessed using combined advanced reliability and structural analysis techniques. Structural analysis explicitly includes deterioration mechanisms resulting from corrosion such as reinforcement area reduction, concrete cracking and bond deterioration.

*Corresponding author

Email address: joan.ramon.casas@upc.edu (Joan R. Casas)

The First Order Reliability Method, combined with a Response Surface algorithm, is used to compute the reliability index for a wide range of different corrosion levels, resulting in a fragility curve. Finally, structural robustness is computed and discussed based on the obtained results. Robustness comparison of different structures can then be used to determine structural types more tolerant to corrosion and these results can be used for maintenance and repair planning.

Keywords: Robustness, Reliability, Damage, Reinforced Concrete, Corrosion

1. Introduction

Maintaining safety and serviceability of existing structures and bridges by making better use of available resources is one of major challenges of transportation agencies in most developed countries since the number structure reaching the design life-time is growing year after year. Strategies, as giving priority to the poorest condition, are clearly insufficient as do not take advantage of structural robustness and tolerance to damage. Currently, decision on maintenance and repair are reactive and based, mostly, on the results of visual inspection and the resulting condition index. The condition index is a convenient indicator of the deterioration of a structure, but provides little information regarding the structural safety, as neither the initial (intact) safety nor the impact of deterioration on safety is considered. Experience has shown that different structures can, for similar deterioration levels, present significantly different safety reductions and safety levels, with a dramatic effect on the need to repair and on the optimal allocation of funds

16 in a network.

17 This paper presents a framework to assess robustness of structures under
18 deterioration. Considering that a detailed safety assessment of every exist-
19 ing structure is impossible due to financial limitations and to the uncertainty
20 related to the real deterioration, the robustness concept proposed herein can
21 serve as an approximated measure of the mean loss in safety independent of
22 the deterioration level. Although a robustness analysis is also complex, the
23 robustness of similar structures is believed to be relatively uniform, allowing
24 a classification of structures in a network based on the detailed analysis of
25 a limited number of structural typologies. This classification can be used in
26 conjunction with the observed or predicted condition state to define the need
27 or urgency of maintenance, considering explicitly the structural properties of
28 a particular structure. This allows a clear distinction between structures
29 which, although presenting similar deterioration levels in specific main com-
30 ponents, have very different safety levels as a result of different geometry or
31 critical failure paths, among others.

32 Focus is also given to reinforced concrete structures (due to representa-
33 tiveness of this structural type worldwide) under reinforcement corrosion as
34 this is one of the major causes of structural deterioration.

35 **2. Structural robustness**

36 Research on robustness has focused on extreme events, such as terrorist
37 attacks. However, the concept can also be very useful in the context of
38 structural aging and deterioration, in particular in the asset management
39 field. Robustness of some structural types can be a crucial to plan and

40 design future infrastructures, requiring less repair and maintenance actions
41 during service lifetime.

42 In what respects to corrosion of reinforced concrete structures, although
43 the mechanisms responsible for rebar corrosion are relatively well known [1],
44 the prediction of future deterioration is associated with very large uncer-
45 tainty. For this reason, deterioration of reinforced concrete structures can be
46 analyzed in a robustness framework, considering corrosion as unpredictable
47 and assuming levels within a wide range. This approach is useful for both new
48 and existing structures, as it indicates, on one hand, the structural designs
49 less susceptible to corrosion and, on the other hand, the existing structures
50 for which higher whole life repair costs can be expected.

51 Although robustness is a desirable property, a consensual definition and
52 a framework to assess it still do not exist [2]. Significant work has been done,
53 in particular under COST¹ Action TU-0601 - Robustness of Structures, but
54 no unanimous methodology has yet been found.

55 Some authors suggest robustness to be a structural property [3, 4, 5, 6]
56 while for others robustness depends also on the surrounding environment
57 [7]. In this case, Robustness is a much broader concept, since it accounts
58 with indirect consequences of failure which depend on several aspects such
59 as social and economical. A deep discussion on the robustness concept can
60 be found in [6].

61 In this paper the perspective of robustness being a structural property is
62 adopted, in order to characterize the damage tolerance of existing structures

¹COST - European Cooperation in the field of Scientific and Technical Research

63 to deterioration. The proposal of [6] is considered since it is sufficiently
64 generic to be applied to most structural types and damage scenarios and
65 can be applied in a probabilistic or deterministic framework. Robustness
66 is defined as a structural property which measures the degree of structural
67 performance remaining after damage occurrence. This relation can take many
68 different forms, depending of the limit state (from service to ultimate limit
69 state) that is adopted in the structural evaluation. Damage can vary from
70 simple degradation to a more serious damage scenario as a local failure.

71 In order to assess robustness, it is fundamental to define a measure of
72 structural performance f and a damage D causing performance decrease.
73 The next step is to define the performance function of the damaged structure
74 $f(D)$ for the complete damage spectrum. The maximum value of damage
75 in the spectrum corresponds to the maximum expected loss of performance
76 during service life. This is important when comparing robustness of different
77 structural types, where the performance profile can be highly different as a
78 function of the damage level or, alternatively, the service life. In the final
79 step, both damage and performance indicator are normalized and the the
80 robustness indicator R_D is computed as follow:

$$R_D = \int_{D=0}^{D=1} f(x)dx \quad (1)$$

81 The robustness index R_D should vary from 0 to 1, respectively for null and full
82 robustness. For null robustness structures, a small level of damage produce
83 a total loss of structural performance and vice-versa.

84 The proposed index, R_D , is a generalization of the proposals of [3, 5] and
85 the damage based measure, $R_{d,int}$ proposed by [2], however with some ad-
86 vantages which appear to solve some of the limitations found in the referred

87 robustness measures. The proposal of [3] is not suitable to deal with con-
88 tinuous damage, which is the case of reinforcement corrosion. This problem
89 appears to be solved in the [5] proposal. Although this index considers con-
90 tinuous values for the damage variable, it results in different values for the
91 robustness index, depending on the damage level. These problems have been
92 solved by the proposed index, R_D , by considering normalized and continu-
93 ous values for both structural performance and damage. Additionally, since
94 all the damage domain is integrated, robustness is given by a unique value
95 independently of the damage level. Thus, robustness may result similar for
96 different structures even if one degrades continuously and the other reacts
97 brittle. However, this can be surpassed if a probabilistic approach is used to
98 measure the structural performance.

99 In this paper, the robustness of reinforced concrete structures subjected
100 to corrosion is analyzed. Damage inflicted to the structure is considered to
101 be the corrosion level on the reinforcement measured in terms of rebar weight
102 loss percentage. The difficulties in defining a probabilistic model for hazard,
103 in this case for corrosion, lead to the analysis under a range of corrosion dif-
104 ferent levels. This strategy has been used in seismic engineering for instance,
105 where fragility curves resulting from exposing structures to different earth-
106 quakes intensities, have been used to characterize structural performance to
107 seismic events. However the concept can be extended to a wide range of
108 other hazards, as structural deterioration and in particular to reinforcement
109 corrosion.

110 In this paper, structural performance is measured through the reliability
111 index as this is a consistent measure of structural safety which takes uncer-

112 tainty into account.

113 **3. Corrosion of reinforced concrete structures**

114 *3.1. Corrosion process*

115 When reinforced concrete is exposed to environmental conditions, steel
116 bars corrosion and iron oxides formation are likely to occur due to the ener-
117 getic potential of the iron-carbon alloy. The iron oxides resulting from the
118 corrosion reaction do not have mechanical properties comparable to those
119 of steel and exhibit volume increase which can go to seven times the origi-
120 nal steel volume. The final result is the occurrence of several deteriorating
121 mechanisms which lead to a deterioration of the structural capacity.

122 During the lifetime of a reinforced concrete structure two periods concern-
123 ing corrosion can be distinguished [8]: the initiation period, respecting to the
124 stage where reinforcement is protected by a thin oxide layer. Within this pe-
125 riod corrosion takes place at a negligible rate and no deterioration effects are
126 expected. The second phase, the propagation period, starts when concrete
127 cover is contaminated and the passive oxide layer is destroyed. This results
128 in increased corrosion rate and deterioration of the structure condition.

129 Steel depassivation occurs mainly due to concrete carbonation and chlo-
130 rides contamination, typical of industrial and maritime environments, re-
131 spectively. In the first case, corrosion is likely to occur uniformly, along steel
132 bars length, while in the second case corrosion tends to be more localized and
133 pronounced, also called pitting corrosion. In both cases several deterioration
134 mechanisms are expected to aggravate the structure condition: reinforcement
135 effective area reduction; ductility reduction of steel bars; concrete cracking

136 and spalling of concrete; bond degradation between steel bars and surround-
137 ing concrete. The influence of these mechanism on the structural behavior
138 depends on several factors such as type of corrosion, reinforcement ratio, con-
139 crete strength, loading, cross section geometry, among others [9]. In general,
140 steel bars effective area and ductility reduction are of more concern in cases
141 of localized or pitting corrosion [10, 11], while concrete cracking and spalling
142 and debonding effect play a more deteriorating role in cases of general cor-
143 rosion [12, 13, 14, 15].

144 Ductility reduction of steel bars is partly due to a chemical transformation
145 of the steel occurring during corrosion process, known as *hydrogen embrittle-*
146 *ment* [16, 17] and partly due to a localization phenomenon resulting from non
147 uniform corrosion [18]. The latter can explain the reason behind ductility
148 reduction of steel bars have been considered specially concerning in cases of
149 pitting corrosion. In these cases however, concrete cracking and spalling and
150 debonding of reinforcement are, in general, not critical, as steel bars can be
151 anchored in less corroded and non cracked zones [19]. However, if corrosion
152 attacks all bar length, spalling of concrete cover is likely to occur and loss of
153 bond between steel bars and concrete, compromising the composite behavior
154 of both materials, is expected. [20] have concluded the effects of localized and
155 generalized corrosion to be potentially more hazardous for bending ultimate
156 and service limit states of highway bridges, respectively. However, is must
157 be noted that the authors have assumed perfect anchorage of reinforcement
158 in the abutments. Even if hooks are provided at reinforcement ends, anchor-
159 age can be greatly impaired by the existence of lapped joints reinforcement
160 [21]. Additionally, it must be noted that corrosion rate is usually increased

161 in zones of reinforcement concentration or where it is bent. According to
162 [12] and [13] reinforcement debonding is the main cause of impaired flexural
163 behavior, if corrosion is found to be generalized and uniform.

164 This paper focus in cases of generalized corrosion. Localized and pitting
165 corrosion are outside the scope of the present paper. For sake of simplicity,
166 only the effects of concrete cracking and spalling, debonding of steel bars
167 and reinforcement effective area reduction will be considered from this stage
168 onwards. Reinforcement impaired ductility and reduction of steel strength,
169 including the spatial variability of corrosion, are not considered herein, al-
170 though it is recognized, and as suggested by [10, 11, 22], that these are
171 factors of paramount importance in cases of localized corrosion, which is not
172 the present case.

173 *3.2. Methodology*

174 As discussed in the previous section, to adequately model the effects of
175 generalized corrosion it is necessary to take into account some undesirable
176 consequences of the oxidation process of rebars, including reinforcement net
177 area reduction and expansion due to corrosion products accumulation. This
178 last phenomenon leads to damage, cracking and splitting of the surround-
179 ing concrete and degradation of steel-concrete bond, responsible for stress
180 transfer between both materials.

181 In order to model all these effects, an advanced Finite Element methodol-
182 ogy was used coupled with advanced constitutive models for modeling mate-
183 rials. Its capability to reproduce the behavior of corroded reinforced concrete
184 was demonstrated by comparing numerical results with results obtained ex-
185 perimentally [23]. The methodology employed considers a two-step analysis.

186 In the first step a finite element analysis of the structure cross section is car-
187 ried out, simulating the formation and accumulation of corrosion products
188 as an expansion of steel bars. In this phase, steel bars are modeled using
189 a linear elastic law and are coupled to concrete through an interface model
190 that regulates the shear stress transference between the two materials. For
191 concrete, an isotropic continuum damage model is used enriched with kine-
192 matics provided by the strong discontinuities theory [24]. The combination of
193 these two approaches, for modeling concrete behavior, allows the simulation
194 of crack development caused by corrosion and expansion of rebars.

195 In the second step, results obtained during the cross section analysis are
196 then used to build a 2D structural model of the corroded structure used to
197 assess the impaired structural capacity. Reinforced concrete is modeled by
198 means of a composite material constituted by a matrix, representing concrete,
199 mixed with long fibers which represent steel bars, as proposed by [25]. This
200 is the main difference from the modeling strategy proposed by [23]. Whereas
201 [23] used a mesoscopic approach for the 2D longitudinal model, using different
202 finite elements for concrete, reinforcing bars and interface. In the homoge-
203 nized model used herein, a unique composite finite element is enriched to
204 reproduce the composite behavior of all the components. As an advantage,
205 the homogenized model requires much less computational resources, due to
206 the smaller size of the numerical model. This is an important aspect in this
207 case, since a large number of different analyses are required to perform the
208 fragility curves. Additionally, the homogenized model seems to reproduce
209 better the global structural behavior since the interface between concrete
210 and steel bars is implicitly considered. In the mesoscopic approach, bond

211 effect is reproduced using interface elements. In this manner, results can be
212 affected by the mesh size, usually resulting in a less stiff global behavior.

213 3.3. Cross section analysis

214 This section depicts results obtained in the first step of the corrosion anal-
215 ysis methodology, obtained for a rectangular section (0.20m×0.40m) with
216 mean values properties of a C30/37 concrete and 2 ϕ 10 and 2 ϕ 20 reinforce-
217 ment steel bars (S400 grade) placed at the upper and bottom section surfaces,
218 respectively. Corrosion was simulated considering a volumetric expansion of
219 steel bars, with similar penetration rates on both bars. Resulting iron oxides,
220 as suggested by [26], were considered incompressible and to occupy twice the
221 initial iron volume. Figure .1 shows the effect of corrosion at a cross section
222 level. Figure .1 (a) shows damage map, d , on concrete due to expansion
223 of steel bars for a corrosion penetration depth, $X = 0.5\text{mm}$, which corre-
224 spond to an area percentage lost of $X_{P1} = 10\%$ and $X_{P2} = 20\%$ for bottom
225 and top reinforcement, respectively. Damage $d = 1$ means concrete had lost
226 all strength and cracking is eminent. Figure .1 (b) shows the correspond-
227 ing isodisplacement lines which concentration indicates crack development
228 as shown in Figure .1 (c).

229 [Figure 1 about here.]

230 Figure .2 shows width evolution of cracks (a) to (e) as corrosion increases.
231 Cracks (a) and (e) are those reaching the range of visible cracks ([0.1-0.2]mm)
232 for a $X_{P_{1/2}} = 1 - 2\%$, therefore consistent with experimental results [9].
233 Figure .2 shows that, for corrosion $X_{P_{1/2}} > 5 - 10\%$, cracks width increase
234 linearly and no additional cracks were detected. This allow the definition of

235 the effective concrete cross section as shown in Figure .1 (d). For sake of
236 simplicity, corrosion of transverse reinforcement was neglected [20], although
237 it is recognized, on one hand the respective positive confinement effect, and
238 on the other hand the additional negative contribution for the cross section
239 deterioration.

240 [Figure 2 about here.]

241 *3.4. Structural Analysis*

242 Results obtained for the cross section analysis were used to build a 2D
243 structural model of the corroded structure. A simply supported 5.0m span
244 beam was used to illustrate the proposed methodology. Reinforced concrete
245 was modeled by means of a composite material constituted by a matrix,
246 representing concrete, mixed with long fibers which represent steel bars, as
247 proposed by [25]. Three types of composite material needed to be considered
248 (see Figure .3): concrete cover (unreinforced plane concrete); concrete on
249 the beam's web, transversely reinforced; and concrete surrounding flexural
250 bars, longitudinally reinforced. As for the cross section analysis, and in order
251 to be able to model crack development, in the longitudinal model the finite
252 elements were also enriched with the strong discontinuities kinematics [24],
253 and for concrete the isotropic continuum damage model was adopted [27].

254 [Figure 3 about here.]

255 For the embedded fibers, the objective was to simultaneously model rein-
256 forcement behavior and debonding effect, resulting from corrosion. In order
257 to achieve such goal, the slipping-fiber model proposed by [25] was adopted,

258 which considers slipping-fiber ϵ^f strain as the sum of the fiber mechanical
259 deformation and the deformation of interface.

260 [Figure 4 about here.]

261 Assuming a two-component serial system constituted by the fiber and the
262 interface, the corresponding slipping-fiber stress σ^f is identical to the stress of
263 each component. On both cases the stress-strain relation can be obtained via
264 an one-dimensional elasto-plastic hardening/softening model. The resulting
265 constitutive behavior, for the slipping-fiber, is also an elasto-plastic model
266 with the following characteristics:

$$\sigma_y^f = \min(\sigma_y^d, \sigma_y^i) \quad (2)$$

267

$$E^f = \frac{1}{\frac{1}{E^d} + \frac{1}{E^i}} \quad (3)$$

268 in which E^d and σ_y^d are the steel Young's modulus and yield stress, respec-
269 tively, E^i is the interface elastic modulus and σ_y^i is the interface bond limit
270 stress. Regard that, when $E^i \rightarrow \infty$ and $\sigma_y^d < \sigma_y^f$, the system provides only
271 the mechanical behavior of the fiber, reproducing a perfect adhesion between
272 concrete and reinforcement bars.

273 For the slipping-fiber model characterization, pullout tests can be per-
274 formed in order to assess the required parameters. In this paper, for the
275 uncorroded state, perfect adhesion between steel bars and concrete is consid-
276 ered and a rigid-plastic behavior for the interface is adopted. This hypoth-
277 esis may be considered acceptable since it is considered that the anchorage
278 lengths are respected and only ultimate limit states related to structural ca-
279 pacity are under analysis. For corroded states, the bond limit stress σ_y^i was

280 considered lower than the reinforcement yielding stress σ_y^d , and depending on
 281 the corrosion level X_p . This means that perfect adhesion it is not valid for
 282 the corroded states, as suggested by several researchers [28, 13, 14, 29, 15].

283 In order to characterize bond strength reduction as a function of the
 284 corrosion level the *M-pull* model proposed by [30] was adopted. This is
 285 an empirical model, based on several author's experimental tests, thus the
 286 following results must me watched carefully. The *M-pull* gives the normalized
 287 bond strength reduction depending on the corrosion level:

$$\frac{\sigma_y^i(X_p)}{\sigma_y^i(X_p = 0)} = \begin{cases} 1.0 & \text{if } X_p \leq 1.5\% \\ 1.192 \cdot e^{-0.117X_p} & \text{if } X_p > 1.5\% \end{cases} \quad (4)$$

288 To build the 2D structural longitudinal model of the deteriorated struc-
 289 ture, it was necessary to import the results obtained for the cross section
 290 corrosion analysis (see Figure .5 (a)). As referred, special attention was
 291 given to crack pattern, *i.e.*, when a crack crossed two cross section faces,
 292 the smaller section part was considered disconnected from the section core
 293 (see Figure .5 (b)) and then, for simplicity, considered with damage $d = 1$
 294 (see Figure .5 (c)). In this case, and as observed in the previous section,
 295 for advanced corrosion stages, concrete corners at both beam's top and bot-
 296 tom tended to split from the section core. The next step was to divide the
 297 cross section into thin horizontal slices and compute the average damage, d ,
 298 for each slice (see Figure .5 (d)). Finally the damage values for each slice,
 299 as shown in Figure .5 (e), were projected on the 2D longitudinal structural
 300 model (see Figure .5 (f)) defining the deteriorated structure.

301

[Figure 5 about here.]

302 **4. Reliability Analysis**

303 As previously referred, the reliability index, β , is the structural perfor-
 304 mance indicator chosen to assess robustness since it is a consistent measure
 305 of safety. However, the reliability of a corroding existing structure is a time-
 306 dependent problem, which can be expressed by the following equation:

$$P_f(t) = \int_{G[X(t)]} f_{X(t)}[X(t)]dx(t) \quad (5)$$

307 where $P_f(t)$ is the instantaneous probability of failure at time t , $X(t)$ is
 308 the random variables vector, $G[X(t)]$ is the limit state function and $f_{X(t)}$ the
 309 joint probability density function of the random variables. The instantaneous
 310 probability of failure can be integrated over an interval of time, $[0; t]$, resulting
 311 in the probability of failure over that time period, $P_f(0, t)$. The random
 312 variables, $X(t)$, are time dependent and, thus, so is $P_f(t)$. The time t at
 313 which the limit state function, $G[X(t)]$, becomes zero is denoted time-to-
 314 failure and equation (5) correspond to a first-passage-probability, assessed
 315 with the out-crossing theory [31]. Time-integrated approaches for solving
 316 equation (5) are much simpler, as lifetime maximums distributions for loads
 317 are used as presented in equation (6)

$$P_f(0, t) = P\left(R(t) \leq S_{max}(t)\right) \quad (6)$$

318 where $R(t)$ is resistance and $S_{max}(t)$ is the maximum load effect for the time
 319 period $[0; t]$. However, as resistance is also time dependent, decreasing with
 320 deterioration, it is extremely unlikely that the maximum load effect coincides
 321 with the time of minimum resistance. By dividing structure lifetime into n
 322 limited time periods, for which resistance can be considered as time invariant,

323 it is possible to approach the first-passage problem by equation (7):

$$P_f(0, t) = 1 - P\left(R_1 \geq S_{max,1} \cap R_2 \geq S_{max,2} \cap \dots \cap R_n \geq S_{max,n}\right) \quad (7)$$

324 where R_i respect to resistance at time interval $[t_{i-1}; t_i]$, considered as con-
 325 stant, and $S_{max,i}$ is the maximum load effects within the same period. De-
 326 spite the independence of $S_{max,i}$ between time periods, the subset of events
 327 presented in equation (7) still show some dependency as a result of the cor-
 328 relation between remaining involved variables. The probability of failure can
 329 finally by estimated using the narrow reliability bounds proposed by [32], as
 330 a comparison between equation (7) and that relative to a serial system can
 331 be established. Thus, if relative short time periods are considered, attend-
 332 ing to the corrosion rate, the probability of failure, given a certain level of
 333 corrosion, can be considered approximately as time-independent. The corre-
 334 sponding reliability index, β , is therefore used herein as the time-independent
 335 performance indicator and equation (1) results in:

$$R = \int_0^1 \frac{\beta(X_P = x)}{\beta(X_P = 0)} dx \quad (8)$$

336 In order to compute the reliability index, the response surface method,
 337 RSM, is used to obtain an explicit approach for the structural response to
 338 allow the First Order Reliability Method, FORM, to be used [33, 34]. To
 339 depict the proposed methodology, the simply supported beam analyzed in
 340 the previous section is being used and considered to support a 0.075m depth
 341 and 1.25m wide concrete deck for pedestrians.

342 The number of random variables considered in this study needed to be
 343 restricted to the most fundamental, due to demanding reliability analysis,

344 sophisticated numerical models, and limited computational resources. Ta-
345 ble .1 shows the distributions and parameters of the six random variables
346 considered in this study. Live load is considered the result of people concen-
347 tration and modeled through a exponential distribution with a 98% quantile
348 of $7.0kN/m^2$ for the maximums distribution in a reference period of 50 years.
349 This results in an exponential rate parameter, λ , of 1.1 and a mean value
350 of $0.90kN/m^2$ for an anual occurrence rate. Thus the probability of failure
351 to be computed will respect to the period of 1 year, and for the usual cor-
352 rosion rates, the resistance of the deteriorating structure can be considered
353 as constant. The width of the deck (1.25m) was considered on the surface
354 loads.

355 [Table 1 about here.]

356 The limit state function, G , is defined as the load carrying capacity cor-
357 responding to a bending failure at mid span, R , minus the acting load, S ,
358 due to self weight and live load. The load effect, S , can be obtained through
359 equation (9)

$$S = \theta_E \times [A_c^{beam} g + W (d_c^{slab} g + q)] \quad (9)$$

360 where W is the deck width equal to 1.25m. A_c^{beam} and d_c^{slab} are the beam cross
361 section and the slab depth, respectively. The resistance can be computed
362 through equation 10:

$$R = \theta_R \times R(f_c, f_y, X_P) \quad (10)$$

363 where $R(f_c, f_y, X_P)$ is the resistance obtained through the corrosion analysis
364 methodology described previously, and explicitly approached by a response
365 surface defined for each design point, d_P .

366 5. Discussion

367 5.1. Reliability analysis

368 Figure .6 shows the reliability index, $\beta(X_P)$, and the respective failure
369 probability, $P_f(X_P)$, evolution with the corrosion level, X_P . The reliability
370 of the intact structure is 3.5 decreasing significantly as corrosion increases,
371 specially in the first 15% of reinforcement area lost. For corrosion levels
372 ranging from 15% to 40%, safety reduction is much less significant, and from
373 this stage onwards almost negligible. The residual reliability is 0.41 attained
374 for 60% of area lost.

375 Figure .6 also shows two additional fragility curves: $\beta(X_P)^*$, where the
376 debonding effect has been neglected; and $\beta(X_P)^{**}$, where only reinforce-
377 ment area reduction has been considered. The comparison between $\beta(X_P)$,
378 $\beta(X_P)^*$ and $\beta(X_P)^{**}$ shows that safety reduction due to reinforcement area
379 reduction is almost linear until corrosion reach about 80%. From this stage
380 onwards, the effective reinforcement area is below the minimum required to
381 avoid structural failure immediately after flexural cracks initiation. Cracking
382 effect is more significant for corrosion above 80%, as from this stage onwards
383 flexural strength is provided by the plain concrete section, which in this case
384 is deteriorated as shown in Figure .1 (d).

385 [Figure 6 about here.]

386 5.2. Robustness assessment

387 Figure .7 shows the normalized performance obtained through the ratio
388 between the reliability of the corroded structure and the intact one, as a
389 function of the normalized damage, in this case considered as the corrosion

390 level on bottom reinforcement. Although results in Figure .6 are referred
391 to penetration attack depths up to the steel bar radius, in Figure .7 the
392 maximum damage is limited to 50%, as for existing structures such level of
393 deterioration would trigger a repair action.

394 [Figure 7 about here.]

395 Robustness computed according to (8) results in $R = 28\%$, showing that
396 tolerance to generalized corrosion is relatively low and safety reduction should
397 always be a concern. This is a result of the lack of redundancy of a simply
398 supported beam, but also of the absence of a second layer of bottom rein-
399 forcement less affected by corrosion.

400 The difference between achieved robustness and the maximum possible
401 value of 100% shows that, in relation to the intact structure, mean safety was
402 decreased in 72% when corrosion. Robustness of the cases where debonding
403 effect has been neglected, and only reinforcement area reduction has been
404 considered, respectively, provide the mean contribution of each deteriorating
405 mechanism. Debonding effect is the main cause of structural deterioration
406 producing a mean safety reduction $\Delta f^1 = 47\%$, followed by reinforcement
407 area lost and then cracking, resulting in $\Delta f^3 = 18\%$ and $\Delta f^2 = 7\%$, respec-
408 tively.

409 5.3. Decision making based on robustness

410 Figure .8 shows the beam time-dependent probability of failure $P_f(0, t)$,
411 referred to the time period $[0, t]$, and considering a corrosion progression of
412 1% annually. The initiation period has been neglected and the time $t = 0$
413 respects to the onset of corrosion. The lower and the upper bounds of the

414 probability of failure resulted very narrow and overlapped in Figure .8 as weak
415 dependency was found between different time periods. Figure .8 also shows
416 the time-dependent probability of failure for a similar beam but considered
417 protected against corrosion, $P_f(0, t)^{***}$. Under the hypothesis of having a full
418 effective protection, in this case robustness would result equal to 100% since
419 no deterioration would be expected. Thus, if a minimum safety threshold is
420 defined for operating structures within a management system, the compar-
421 ison between the unprotected and the protected beam shows that the time
422 for the first intervention should be smaller for the unprotected structure due
423 to lack in robustness. Figure .8 also shows the time-dependent probability of
424 failure when neglecting debonding effect, $P_f(0, t)^*$, and considering only the
425 effect of reinforcement area reduction $P_f(0, t)^{**}$. As mentioned, debonding
426 is the major cause for impaired robustness thus with major impact on the
427 time-dependent probability of failure.

428 [Figure 8 about here.]

429 Similarly, a longer time between periodic inspections could be adopted
430 depending on robustness. Figure .9 shows the time-dependent probability
431 of failure, for the same cases of Figure .9, given the observed corrosion level
432 at the inspection time and within the period between inspections, consid-
433 ered herein, and for exemplification proposes, equal to 3 years, $P_f(3y)$. As
434 observed, the probability of failure within the time between inspections is
435 constant for the beam protected against corrosion due to full robustness. For
436 the unprotected beam, the probability of failure increases with the corrosion
437 degree. Therefore a reduction of the time between inspections is required
438 over the beam lifetime.

[Figure 9 about here.]

439

440 **6. Conclusions**

441 In this work, a probabilistic framework for the evaluation of structural
442 robustness of structures, subject to continuous damage, is presented. In this
443 framework, damage is defined in terms of an unpredictable continuous vari-
444 able, making this robustness index particularly suitable for structural man-
445 agement systems allowing the analysis and comparison of different structural
446 types with the final objective of defining those requiring more and prior main-
447 tenance. The results obtained showed the ability of the proposed index to
448 characterize the robustness of a structure, from a structural viewpoint, in
449 a single indicator, independently of the structural safety of the undamaged
450 structure. Robustness of the presented example resulted in 28% which shows
451 the structure tolerance to generalized reinforcement corrosion. The mean
452 performance lost is 72% of which 47%, 18% and 7% are caused by bond
453 deterioration, reinforcement area reduction and concrete cover cracking, re-
454 spectively. The comparison with a similar beam but fully robust (due to a
455 corrosion protection), shows that the unprotected beam, thus less robust, re-
456 quires sooner maintenance and shorter periods between periodic inspections.
457 For the sake of simplicity in introducing the concept of robustness index, the
458 example presented in this paper corresponds to a single simply-supported
459 beam. However, it is known that in statically indeterminate structures dam-
460 age effects include a redistribution of internal forces. How this redistribution
461 affects the final value of robustness because of redistribution of stresses and
462 activation of alternative loading paths, is the subject of a future paper where

463 the example of a complete deck with various girders is presented.

464 **Acknowledgments**

465 The authors would like to acknowledge Cost Action TU-0601, Fundação
466 para a Ciência e Tecnologia scholarship SFRH/BD/45799/2008 and Re-
467 search Project PTDC/ECM-COM/2911/2012 and UNIC - Research Center
468 in Structures and Construction of the Universidade Nova de Lisboa and the
469 Spanish Ministry of Education, Research Project BIA2010-16332.

470 **References**

- 471 [1] K. Vu, M. Stewart, Structural reliability of concrete bridges including
472 improved chloride-induced corrosion models, *Structural safety* 22 (4)
473 (2000) 313–333.
- 474 [2] U. Starossek, M. Haberland, Approaches to measures of structural ro-
475 bustness, *Structure and Infrastructure Engineering* 7 (7-8) (2011) 625–
476 631.
- 477 [3] D. M. Frangopol, J. P. Curley, Effects of damage and redundancy on
478 structural reliability, *Journal of Structural Engineering* 113 (7) (1987)
479 1533–1549.
- 480 [4] N. Lind, A measure of vulnerability and damage tolerance, *Reliability*
481 *engineering & systems safety* 48 (1) (1995) 1–6.
- 482 [5] F. Biondini, S. Restelli, Damage propagation and structural robustness,
483 in: *Life-Cycle Civil Engineering: Proceedings of the International Sym-*

- 484 posium on Life-Cycle Civil Engineering, IALCCE'08, Varenna, Lake
485 Como, Taylor & Francis, 2008, p. 131.
- 486 [6] E. S. Cavaco, J. R. Casas, L. A. Neves, A. E. Huespe, Robustness of cor-
487 roded reinforced concrete structures—a structural performance approach,
488 *Structure and Infrastructure Engineering* 9 (1) (2013) 42–58.
- 489 [7] J. Baker, M. Schubert, M. Faber, On the assessment of robustness,
490 *Structural Safety* 30 (3) (2008) 253–267.
- 491 [8] R. Melchers, C. Li, W. Lawanwisut, Probabilistic modeling of struc-
492 tural deterioration of reinforced concrete beams under saline environ-
493 ment corrosion, *Structural Safety* 30 (5) (2008) 447 – 460. doi:DOI:
494 10.1016/j.strusafe.2007.02.002.
495 URL
- 496 [9] F. i. d. b. fib, Bond of Reinforcement in Concrete: State-of-art Report,
497 Bulletin (Fédération internationale du béton), International Federation
498 for Structural Concrete, 2000.
499 URL
- 500 [10] M. G. Stewart, Spatial variability of pitting corrosion and its influence
501 on structural fragility and reliability of rc beams in flexure, *Structural*
502 *Safety* 26 (4) (2004) 453 – 470. doi:DOI: 10.1016/j.strusafe.2004.03.002.
- 503 [11] M. G. Stewart, A. Al-Harthy, Pitting corrosion and structural relia-
504 bility of corroding rc structures: Experimental data and probabilistic
505 analysis, *Reliability Engineering & System Safety* 93 (3) (2008) 373

- 506 – 382, probabilistic Modelling of Structural Degradation. doi:DOI:
507 10.1016/j.ress.2006.12.013.
- 508 [12] A. Almusallam, A. Al-Gahtani, A. Aziz, F. Dakhil, et al., Effect of
509 reinforcement corrosion on flexural behavior of concrete slabs, Journal
510 of materials in civil engineering 8 (1996) 123.
- 511 [13] P. Mangat, M. Elgarf, Flexural strength of concrete beams with corroding
512 reinforcement, ACI Structural Journal 96 (1).
- 513 [14] R. Al-Hammoud, K. Soudki, T. H. Topper, Bond analysis of corroded
514 reinforced concrete beams under monotonic and fatigue loads,
515 Cement and Concrete Composites 32 (3) (2010) 194–203, 00025.
516 doi:10.1016/j.cemconcomp.2009.12.001.
517 URL
- 518 [15] A. Kivell, A. Palermo, A. Scott, Corrosion Related Bond Deterioration
519 and Seismic Resistance of Reinforced Concrete Structures, in: Structures
520 Congress 2012, American Society of Civil Engineers, 2012, pp. 1894–
521 1905, 00001.
522 URL
- 523 [16] R. Schroeder, I. Müller, Stress corrosion cracking and hydrogen embrittlement
524 susceptibility of an eutectoid steel employed in prestressed
525 concrete, Corrosion science 45 (9) (2003) 1969–1983.
- 526 [17] J. Woodtli, R. Kieselbach, Damage due to hydrogen embrittlement and
527 stress corrosion cracking, Engineering Failure Analysis 7 (6) (2000) 427–
528 450.

- 529 [18] R. Palsson, M. Mirza, Mechanical response of corroded steel reinforce-
530 ment of abandoned concrete bridge, *ACI Structural journal* 99 (2).
- 531 [19] J. Cairns, Z. Zhao, Behaviour of concrete beams with exposed reinforce-
532 ment, in: *Proceedings of the Institution of Civil Engineers: Structures*
533 *and Bridges*, Vol. 99, 1993.
- 534 [20] D. V. Val, M. G. Stewart, R. E. Melchers, Effect of reinforcement cor-
535 rosion on reliability of highway bridges, *Engineering Structures* 20 (11)
536 (1998) 1010 – 1019. doi:DOI: 10.1016/S0141-0296(97)00197-1.
537 URL
- 538 [21] Y. Murakami, A. Kinoshita, S. Suzuki, Y. Hukumoto, H. Oshita, In-
539 fluence of lapped splices on residual flexural behavior of rc beams with
540 corrosion of reinforcement, *Concrete Research and Technology* 17 (1).
- 541 [22] M. G. Stewart, Q. Suo, Extent of spatially variable corrosion dam-
542 age as an indicator of strength and time-dependent reliability of rc
543 beams, *Engineering Structures* 31 (1) (2009) 198 – 207. doi:DOI:
544 10.1016/j.engstruct.2008.08.011.
- 545 [23] P. Sánchez, A. Huespe, J. Oliver, S. Toro, Mesoscopic model to simu-
546 late the mechanical behavior of reinforced concrete members affected by
547 corrosion, *International Journal of Solids and Structures* 47 (5) (2010)
548 559 – 570. doi:DOI: 10.1016/j.ijsolstr.2009.10.023.
- 549 [24] J. Oliver, A. Huespe, M. Pulido, E. Chaves, From continuum mechanics
550 to fracture mechanics: the strong discontinuity approach, *Engineering*
551 *Fracture Mechanics* 69 (2) (2002) 113–136.

- 552 [25] J. Oliver, D. Linero, A. Huespe, O. Manzoli, Two-dimensional modeling
553 of material failure in reinforced concrete by means of a continuum strong
554 discontinuity approach, *Computer Methods in Applied Mechanics and*
555 *Engineering* 197 (5) (2008) 332–348.
- 556 [26] F. Molina, C. Alonso, C. Andrade, Cover cracking as a function of re-
557 bar corrosion: Part 2 numerical model, *Materials and Structures* 26 (9)
558 (1993) 532–548.
- 559 [27] J. Oliver, M. Cervera, S. Oller, J. Lubliner, Isotropic damage models and
560 smeared crack analysis of concrete, in: *Second International Conference*
561 *on Computer Aided Analysis and Design of Concrete Structures*, Vol. 2,
562 1990, pp. 945–958.
- 563 [28] A. Almusallam, A. Al-Gahtani, A. Aziz, Effect of reinforcement cor-
564 rosion on bond strength, *Construction and Building Materials* 10 (2)
565 (1996) 123–129.
- 566 [29] H. Yalciner, O. Eren, S. Sensoy, An experimental study on the bond
567 strength between reinforcement bars and concrete as a function of con-
568 crete cover, strength and corrosion level, *Cement and Concrete Research*
569 42 (5) (2012) 643–655, 00038. doi:10.1016/j.cemconres.2012.01.003.
570 URL
- 571 [30] K. Bhargava, A. Ghosh, Y. Mori, S. Ramanujam, Corrosion-induced
572 bond strength degradation in reinforced concrete-analytical and empiri-
573 cal models, *Nuclear Engineering and Design* 237 (11) (2007) 1140–1157.

- 574 [31] R. E. Melchers, Structural reliability analysis and prediction, John Wiley
575 & Son Ltd, 1999.
- 576 [32] O. Ditlevsen, Narrow reliability bounds for structural systems, Journal
577 of structural mechanics 7 (4) (1979) 453–472.
- 578 [33] C. Bucher, U. Bourgund, A fast and efficient response surface approach
579 for structural reliability problems, Structural safety 7 (1) (1990) 57–66.
- 580 [34] H. M. Gomes, A. M. Awruch, Comparison of response surface and neural
581 network with other methods for structural reliability analysis, Structural
582 Safety 26 (1) (2004) 49–67, 00205. doi:10.1016/S0167-4730(03)00022-5.
583 URL

584 **List of Figures**

585 .1 Damage and cracking on beam's cross section due to steel bar
586 expansion. (a) Damage d , for $X_{P_1} = 10\%$, $X_{P_2} = 20\%$; (b) Iso-
587 displacement contour lines; (c) Cracking pattern; (d) Effective
588 cross section. 29

589 .2 Cross section cracks width as a function of the corrosion depth,
590 X , and levels, X_{P_1} and X_{P_2} 30

591 .3 Structural finite element model. 31

592 .4 Slipping-fiber model. 32

593 .5 Coupling cross section and structural analysis: (a)concrete
594 damage map, d ; (b) effective cross section; (c)equivalent dam-
595 age distribution; (d) average damage calculation; (e) average
596 damage distribution; (f) initial damage on structural model. . . 33

597 .6 Reliability index, β , and failure probability, P_f , as a function
598 of the corrosion level, X_P 34

599 .7 Normalized performance as a function of normalized dam-
600 age considering: $\beta(X_P)/\beta(0)$, all three deteriorating effects;
601 $\beta(X_P)/\beta(0)^*$, neglecting debonding effect; $\beta(X_P)/\beta(0)^{**}$, ne-
602 glecting cracking and debonding effects. 35

603 .8 Time-dependent probability of failure considering: $P_f(0, t)$,
604 all three deteriorating effects; $P_f(0, t)^*$, neglecting debonding
605 effect; $P_f(0, t)^{**}$, neglecting cracking and debonding effects;
606 $P_f(0, t)^{***}$, protection against corrosion 36

607 .9 Probability of failure within the period between inspections,
608 considering: $P_f(3y|X_P)$, all three deteriorating effects; $P_f(3y|X_P)^*$,
609 neglecting debonding effect; $P_f(3y|X_P)^{**}$, neglecting cracking
610 and debonding effects; $P_f(3y|X_P)^{***}$, protection against cor-
611 rosion 37

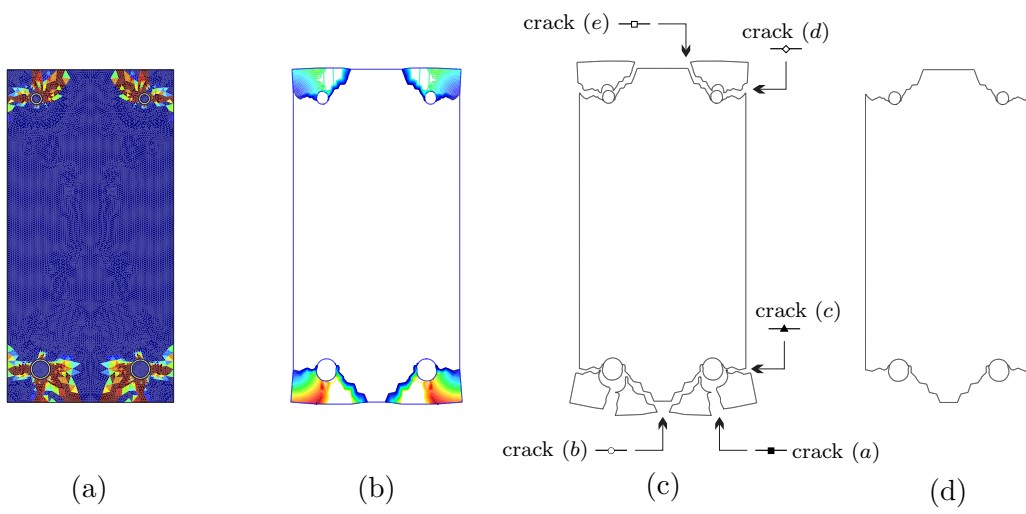


Figure .1: Damage and cracking on beam's cross section due to steel bar expansion. (a) Damage d , for $X_{P_1} = 10\%$, $X_{P_2} = 20\%$; (b) Iso-displacement contour lines; (c) Cracking pattern; (d) Effective cross section.

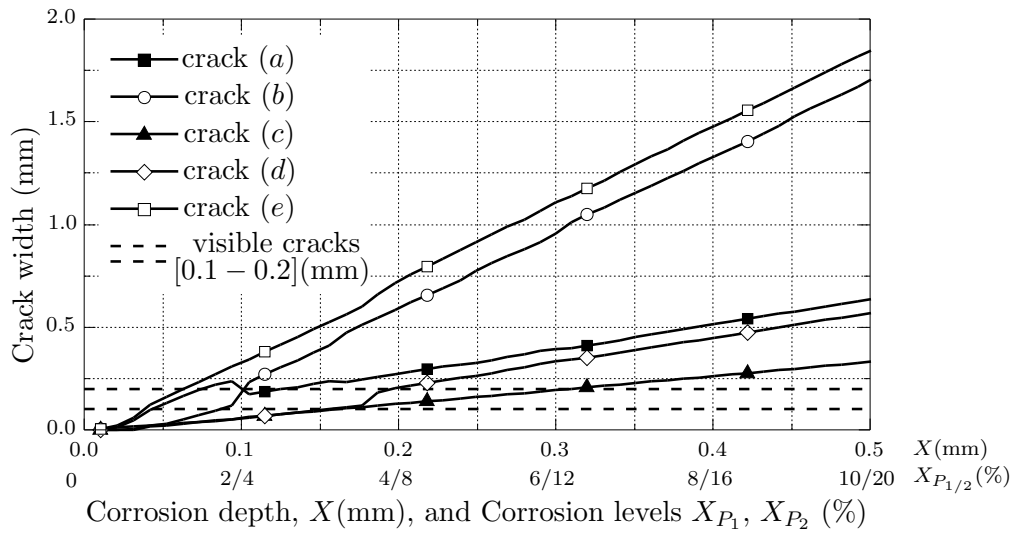


Figure .2: Cross section cracks width as a function of the corrosion depth, X , and levels, X_{P_1} and X_{P_2}

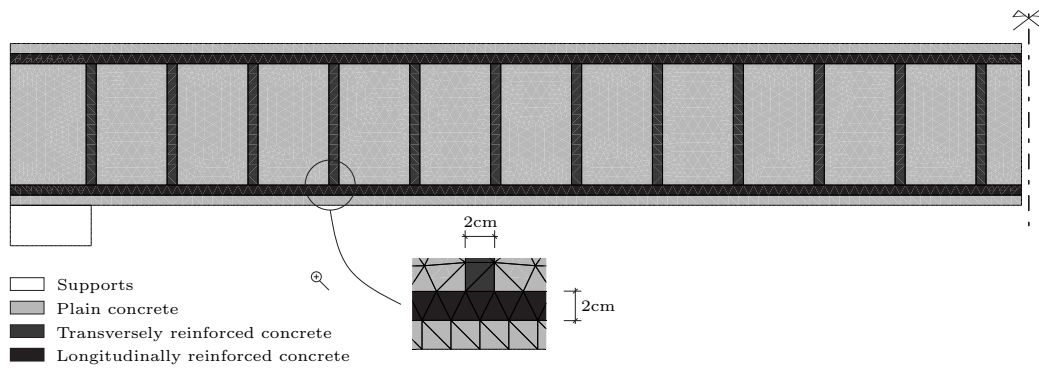


Figure .3: Structural finite element model.

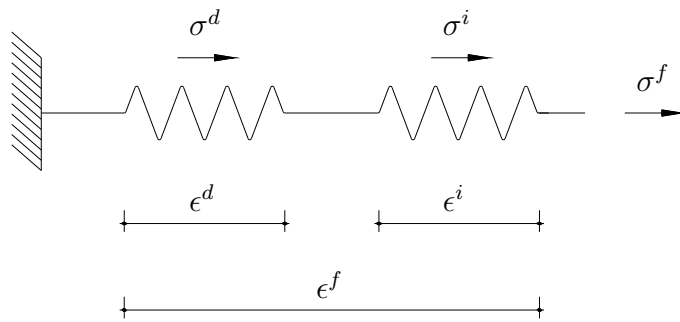


Figure .4: Slipping-fiber model.

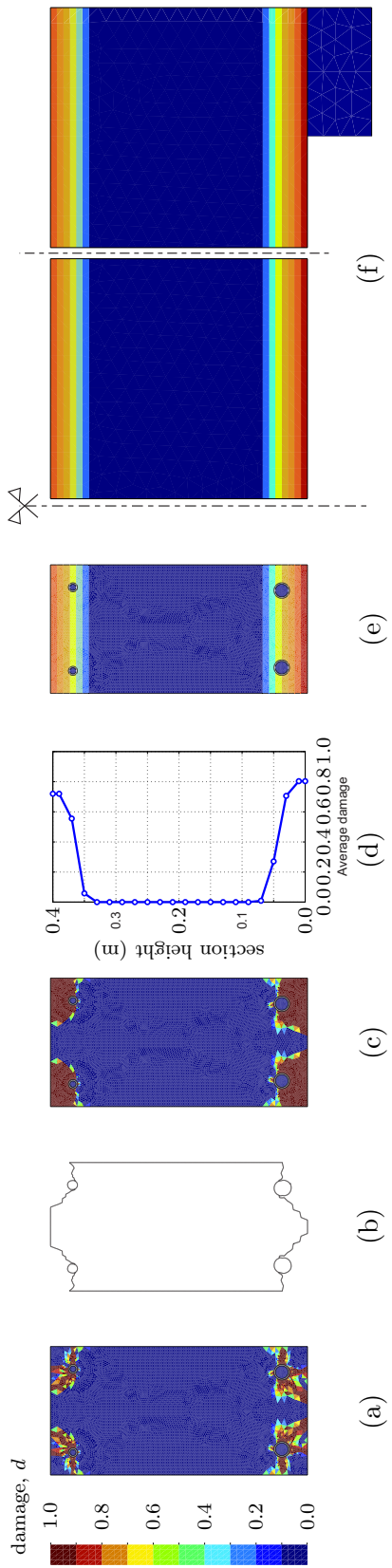


Figure 5: Coupling cross section and structural analysis: (a)concrete damage map, d ; (b) effective cross section; (c)equivalent damage distribution; (d) average damage calculation; (e) average damage distribution; (f) initial damage on structural model.

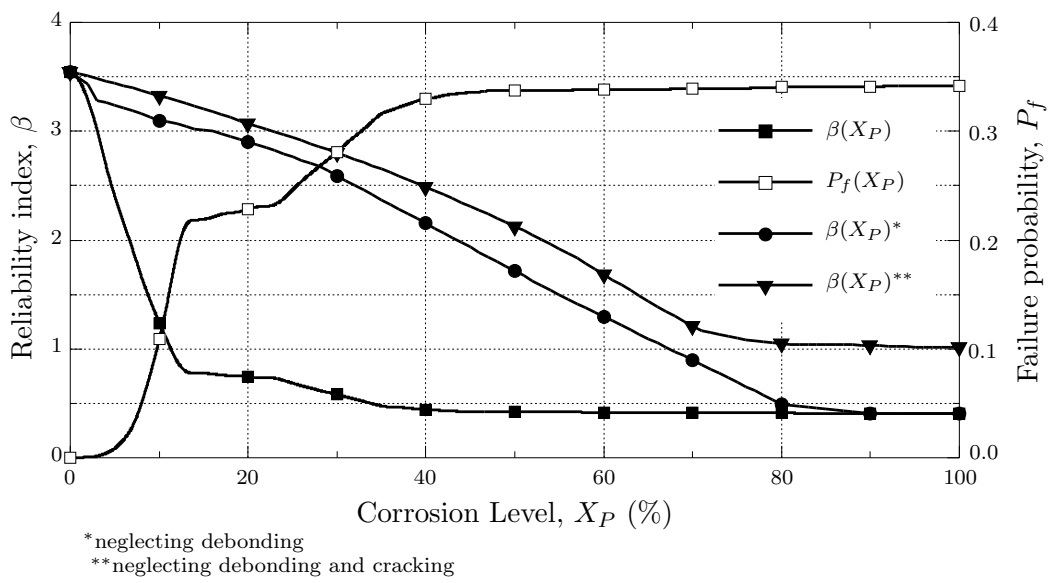


Figure .6: Reliability index, β , and failure probability, P_f , as a function of the corrosion level, X_P .

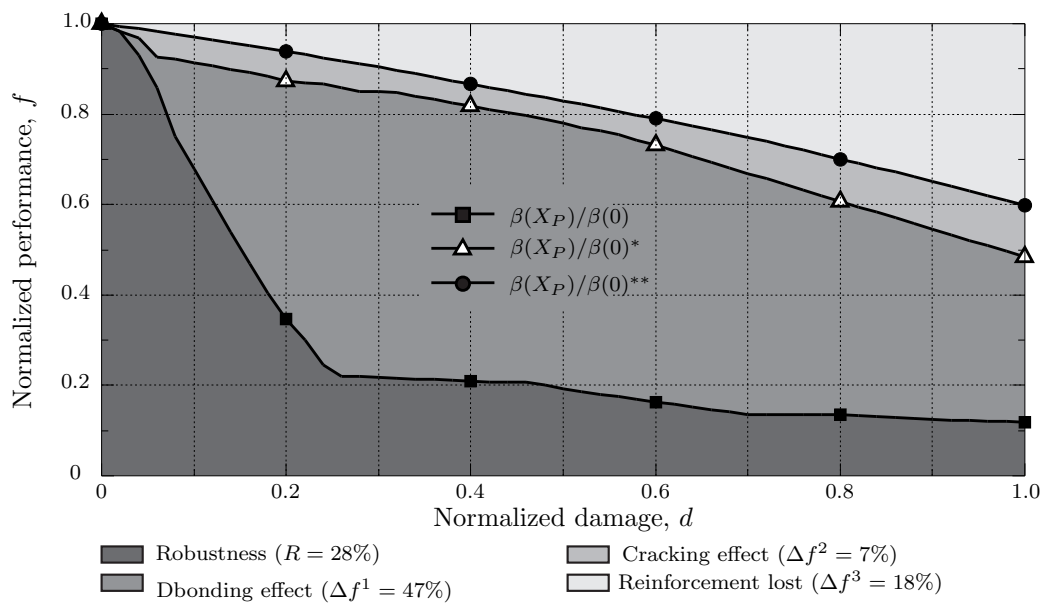


Figure .7: Normalized performance as a function of normalized damage considering: $\beta(X_P)/\beta(0)$, all three deteriorating effects; $\beta(X_P)/\beta(0)^*$, neglecting debonding effect; $\beta(X_P)/\beta(0)^{**}$, neglecting cracking and debonding effects.

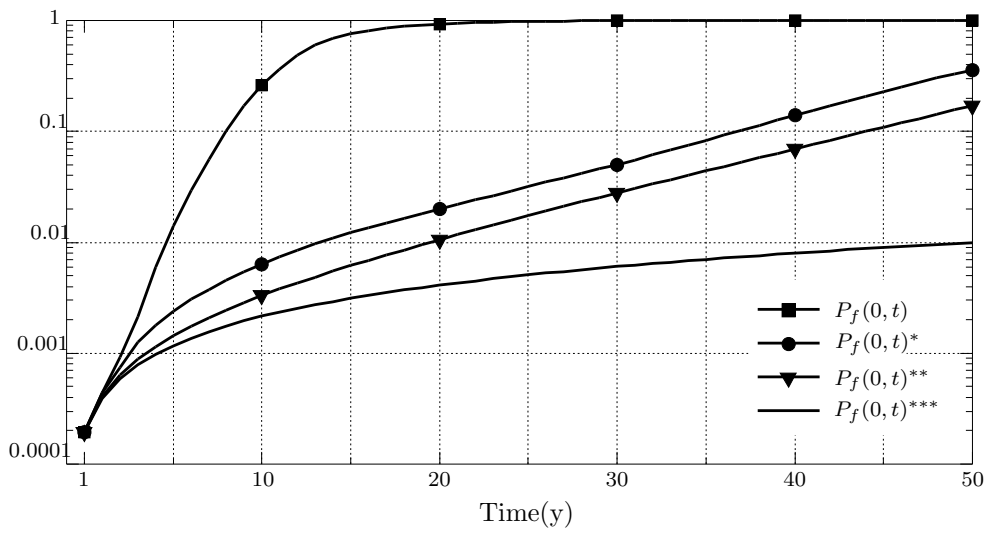


Figure 8: Time-dependent probability of failure considering: $P_f(0, t)$, all three deteriorating effects; $P_f(0, t)^*$, neglecting debonding effect; $P_f(0, t)^{**}$, neglecting cracking and debonding effects; $P_f(0, t)^{***}$, protection against corrosion

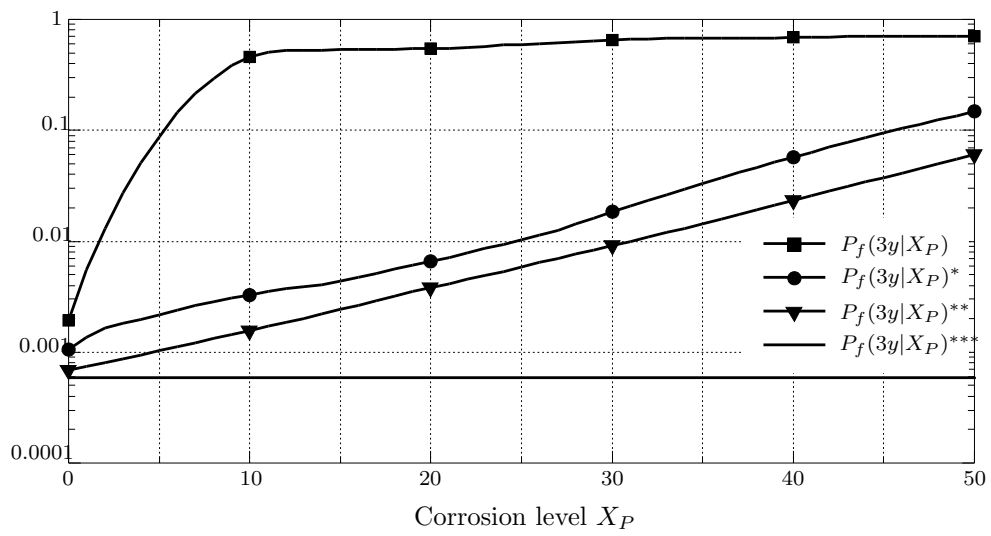


Figure .9: Probability of failure within the period between inspections, considering: $P_f(3y|X_P)$, all three deteriorating effects; $P_f(3y|X_P)^*$, neglecting debonding effect; $P_f(3y|X_P)^{**}$, neglecting cracking and debonding effects; $P_f(3y|X_P)^{***}$, protection against corrosion

612 **List of Tables**

613 .1 Random variables distributions and parameters 39

Table .1: Random variables distributions and parameters

Random Variable	Dist.	Mean	Std. dev.
Concrete strength, f_c	logn	$38.5MPa$	$5.8MPa$
Steel strength, f_y	norm	$460MPa$	$30MPa$
Concrete self-weight, g	norm	$25kN/m^3$	$0.75kN/m^3$
Live loads, q	exp	$0.90kN/m^2$	$0.90kN/m^2$
Resistance model uncertainty, θ_R	logn	1.1	0.15
Load model uncertainty, θ_E	logn	1.0	0.10